

Particle Interactions in Kaolinite Suspensions and Corresponding Aggregate Structures

Vishal Gupta¹, Marc A. Hampton², Jason R. Stokes², Anh V. Nguyen² and
Jan D. Miller^{1,*}

¹Vishal Gupta

Graduate Research Assistant

Department of Metallurgical Engineering, College of Mines and Earth Sciences

University of Utah

135 South 1460 East, Room 412

Salt Lake City, UT 84112, USA

Phone: 801-819-6431

Fax: 801-581-4937

E-mail: Vishal.Gupta@utah.edu

²Marc A. Hampton

Post Doctoral Fellow

School of Chemical Engineering

The University of Queensland

Brisbane, QLD 4072, Australia

Phone: +61 7 3365 3720

Fax: +61 7 336 54199

1 E-mail: m.hampton@uq.edu.au

2
3 ²Jason R. Stokes,
4 Associate Professor
5 School of Chemical Engineering
6 The University of Queensland
7 Brisbane, QLD 4072, Australia

8 Phone: +61 7 336 54361

9 Fax: +61 7 336 54199

10 E-mail: Jason.Stokes@uq.edu.au

11
12 ²Anh V. Nguyen,
13 Professor and BHP Billiton Mitsubishi Alliance (BMA) Chair
14 School of Chemical Engineering
15 The University of Queensland
16 Brisbane, QLD 4072, Australia

17 Phone: +61 7 336 53665

18 Fax: +61 7 336 54199

19 E-mail: anh.nguyen@eng.uq.edu.au

20
21 ^{1,*}Jan D. Miller (Corresponding Author)
22 Chair and Ivor D. Thomas Distinguished Professor of Metallurgical Engineering
23 Department of Metallurgical Engineering

College of Mines and Earth Sciences

University of Utah

135 South 1460 East, Room 412

Salt Lake City, UT 84108, USA

Phone: 801-581-5160

Fax: 801-581-4937

E-mail: Jan.Miller@utah.edu

Abstract

The surface charge densities of the silica face surface and the alumina face surface of kaolinite particles, recently determined from surface force measurements using atomic force microscopy, show a distinct dependence on the pH of the system. The silica face was found to be negatively charged at $\text{pH} > 4$, whereas the alumina face surface was found to be positively charged at $\text{pH} < 6$, and negatively charged at $\text{pH} > 8$. The surface charge densities of the silica face and the alumina face were utilized in this study to determine the interaction energies between different surfaces of kaolinite particles.

Results indicate that the silica face–alumina face interaction is dominant for kaolinite particle aggregation at low pH. This face–face association increases the stacking of kaolinite layers, and thereby promotes the edge–face (edge–silica face and edge–alumina face) and face–face (silica face–alumina face) associations with increasing pH, and hence the maximum shear yield stress at

pH 5-5.5. With further increase in pH, the face–face and edge–face association decreases due to increasing surface charge density on the silica face and the edge surfaces, and decreasing surface charge density on the alumina face. At high pH, all kaolinite surfaces become negatively charged, kaolinite particles are dispersed, and the suspension is stabilized. The face–face association at low pH has been confirmed from cryo-SEM images of kaolinite aggregates taken from suspension which show that the particles are mostly organized in a face–face and edge–face manner. At higher pH conditions, the cryo-SEM images of the kaolinite aggregates reveal a lower degree of consolidation and the edge–edge association is evident.

Keywords: Kaolinite; interaction energy; rheology; cryo-SEM.

Introduction

The rheological properties of concentrated suspensions of clay minerals such as kaolinite $[\text{Al}_2\text{O}_3 \cdot 2\text{SiO}_2 \cdot 2\text{H}_2\text{O}]$ are very important in ceramics, in paper and pulp, in drilling mud, in filtration, in dewatering, and in many other new applications such as clay-polymer nano composites etc [1-3]. Kaolinite particles are naturally pseudo-hexagonal platy shaped ranging from micron to nano size particles. The crystallographic structure suggests that kaolinite particles consist of a silica tetrahedral surface corresponding to the 001 basal plane and an aluminum hydroxide octahedral surface corresponding to the $00\bar{1}$ basal plane as shown in figure 1. Of course, the kaolinite particles have 010 and 110 edge surfaces which are generated as a result of broken covalent bonds. The rheological properties of kaolinite are governed by its surface

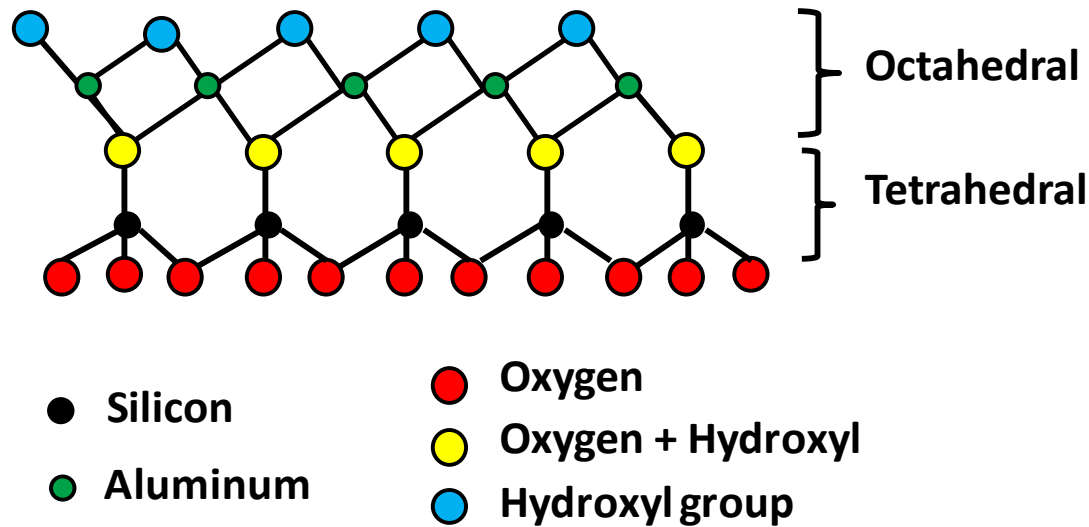


Figure 1: The structure of kaolinite along 010 edge surface showing a silica tetrahedral layer and an alumina octahedral layer.

It is traditionally believed that the 001 and 00 $\bar{1}$ basal plane surfaces of kaolinite particles are negatively charged due to isomorphic substitution of Al^{3+} for Si^{4+} in the silica tetrahedral layer and Mg^{2+} for Al^{3+} in the alumina octahedral layer, whereas the edge surface (010 and 110 plane surfaces) carries a positive or negative charge depending on the pH of the system [4-9]. Following this assumption, several researchers have defined the rheological properties of kaolinite, and have explained the abnormal behavior of a maximum yield stress for kaolinite suspensions at pH 5-5.5 [6-9]. Such a maximum might be expected at kaolinite's iso-electric point of pH < 3 [10, 11]. Johnson *et al.* [7, 8] have gone further in their analysis and explained

1 this abnormal rheological behavior based on the aggregation behavior of kaolinite particles,
2 which is described mainly by edge–face attractions and some face–face attractions. On this basis
3 the maximum shear-yield stress at pH 5.5 was explained.

4
5 The assumption that both basal planes carry a fixed negative charge has only recently been
6 examined experimentally through surface force measurements using atomic force microscopy
7 (AFM) [12]. These colloidal force measurements reveal that the silica tetrahedral face of
8 kaolinite is negatively charged at $\text{pH} > 4$, whereas the alumina octahedral face of kaolinite is
9 positively charged at $\text{pH} < 6$, and negatively charged at $\text{pH} > 8$. The results suggest that the iso-
10 electric point of the silica tetrahedral face is at $\text{pH} < 4$, and that the iso-electric point of the
11 alumina octahedral face lies between pH 6 and 8 [12]. Based on this new finding, Gupta *et al.*
12 [13] determined the interaction energies between different surfaces of kaolinite particles, which
13 showed that the silica face–alumina face association is likely to be dominant for kaolinite particle
14 association at low and intermediate pH conditions. However, the above conclusion of dominant
15 silica face–alumina face association was reached by assuming that the zeta-potential of the edge
16 was a linear combination of the zeta-potentials on silica and alumina surfaces [14]. The
17 assumption for edge surface zeta-potential will be discussed later in this study. It seems that the
18 edge surface zeta-potential for kaolinite is under-estimated, and that an experimental technique
19 such as potentiometric titration should be considered in the analysis of kaolinite surface
20 potentials.

21
22 Several researchers have examined images of flocculated kaolinite suspensions using electron
23 microscopy to determine the aggregate structure, and relate these observations to rheological

1 properties. The earliest significant discussion of clay fabric was given by Terzaghi in 1925 (see
 2 O'Brien [15]) in which the structure of cohesive soils was discussed with regards to adhesion
 3 between adjacent minerals. Casagrande [16] presented a theory for a honeycomb structure in
 4 soils. Idealized drawings of clay fabric forming a card-house or honeycomb structure have been
 5 proposed [5, 17-19]. Rosenqvist [20, 21] published the first electron micrograph of freeze-dried
 6 samples of undisturbed marine Oslo blue clay and supported the idea of card-house arrangement
 7 in the undisturbed sediment. O'Brien [15] examined the fabric of kaolinite in distilled and
 8 slightly saline water, and found that the fabric is dominated by a 3-dimensional network of
 9 twisted chains of face-face oriented flakes having the appearance of a stair-stepped cardhouse.
 10 Recently, Zbik *et al.* [22] investigated the structure of kaolinite aggregates at pH 8 during
 11 sedimentation experiments using cryogenic-scanning electron microscopy (cryo-SEM). They
 12 found that the kaolinite aggregates initially show edge-face and edge-edge association, which
 13 rearranges from edge-edge chains to more compact face-face associations during settling. In
 14 another study, Zbik and Frost [23] observed differences in the physical behavior of a number of
 15 kaolinite clays from Birdwood and Georgia. For example, SEM micrographs of the Birdwood
 16 kaolinite aggregates show the predominance of stair step edge-edge contacts forming a spacious
 17 cell structure, whereas Georgia kaolinite aggregates display edge-face contacts building a card-
 18 house structure. From these studies it is suggested that kaolinite clays are very complex and each
 19 kaolinite should be considered separately. It is evident that each kaolinite from different sources
 20 must be characterized and detailed examination may be necessary to determine the aggregate
 21 structures at low, medium and high pH values.
 22

It is the objective of this paper to utilize the surface charge information on the face surfaces and edge surfaces of kaolinite in order to understand the structure of kaolinite suspensions and corresponding rheological behavior. Furthermore, the influence of particle aspect ratio and electrical double layer thickness is investigated with regard to the aggregation behavior of kaolinite particles. Finally, cryo-SEM images were used to examine the modes of particle association (face–face, edge–face, and edge–edge).

Materials and Methods

Sample Preparation. A clean English Kaolin (Imerys Inc., UK) was obtained from the St Austell area in Cornwall, UK. The sample was cleaned with water only using elutriation to achieve classification at a size of less than 2 μm . No other chemical treatment was used. Further details about the kaolinite extraction and preparation are given in the literature [24]. The kaolinite suspension was prepared in high purity Milli-Q water (Millipore Inc.). The resistivity of the water was 18.2 M Ω -cm in all experiments. Potassium chloride (1 mM solution) was used as background electrolyte for surface force measurements. The pH was adjusted to its desired value using 0.1 M HCl or 0.1 M KOH solutions. All chemicals used were of ACS reagent grade.

X-ray diffraction (Bruker AXS, Inc., Madison, WI, USA) analysis conducted on the kaolinite sample confirmed that kaolinite is the dominant mineral phase. Energy dispersive X-ray spectroscopy (FEI, Hillsboro, Oregon, USA) analysis of the kaolinite sample showed nearly 1:1 atomic distribution of aluminum (7.98%) and silicon (7.95%) with trace amounts of potassium

(0.35%), calcium (0.08%) and iron (0.15%). Other details about the purity of kaolinite are provided elsewhere [12].

The kaolinite particles with a median diameter of 600 nm and median thickness of 11.2 nm in 1 mM KCl solution were used in this study, unless otherwise mentioned. The median diameter and thickness were determined from the imaging of at least 150 kaolinite particles using atomic force microscopy. The kaolinite particles were air-dried on a thin sheet of mica and an image of the particle was obtained using the contact mode imaging technique. Section analysis was then conducted to obtain information about the diameter and thickness of the particle. The details are provided in the Supporting Information.

Aggregate Size. The aggregate size of kaolinite particles in suspension at desired pH values was determined using photon correlation spectroscopy (PCS). In a PCS experiment, the fluctuation of scattered light from the particles by their Brownian motion is collected at a scattering angle of 90° by an optical fiber, and detected by a photo-electric detector. The amplified signal from the photo-electric detector is fed into an autocorrelator for computing the intensity autocorrelation function. This autocorrelation function is used to determine the relaxation of intensity fluctuations, which in turn is related to translational diffusion coefficient of the particles. Particle size (equivalent spherical diameter) is then determined from the diffusion coefficient of the particles.

Kaolinite suspensions (4%) were prepared in 1mM KCl solution at pH 9.0, sonicated for 5 minutes and stirred for 1 hour for complete dispersion. After conditioning, 50 mL of the

suspensions was taken in a volumetric flask and adjusted to the desired pH of 3, 5, 7 and 9 using 0.1 M HCl or 0.1 M KOH solutions. A small amount of kaolinite suspensions (1 mL) was taken at each pH into a cuvette for PCS analysis. Each experiment was replicated three times and the average aggregate size was determined.

Cryo-SEM. Kaolinite suspensions (1%) were prepared in 1 mM KCl solution (100 mL). About 15 ml of the sample was taken in a vial and adjusted to pH 3, 5, 7 and 9 using 0.1 M HCl or 0.1 M KOH solutions. The suspension was left overnight for conditioning. The sample was hand-shaken, and then a few microliters of the suspension were taken in a small metal rivet sealed with glue at one end. The sample was immediately plunged into a liquid N₂ slush using the Oxford LN₂ slush freezing apparatus for freezing the water without allowing crystallization, i.e. vitrifying. Vitrified samples were placed onto the liquid nitrogen-cooled specimen stage of the field emission scanning electron microscope Philips XL30 FESEM with Oxford CT 1500 Cryo stage. The sample was fractured under vacuum and a small amount of vitrified H₂O was sublimed off by raising the stage temperature to −90 °C for 10 minutes to expose the aggregate structure, then lowering back to −180 °C. Finally, the sample was coated with platinum before SEM imaging.

DLVO Model

Interactions between kaolinite particles were characterized by the (Deryaguin-Landau-Vervey-Overbeek) DLVO model, which considers the sum of electrostatic and van der Waals forces. An

appropriate form for the van der Waals interaction energy per unit area (E^{vdW}) between two planar surfaces of thickness δ_1 and δ_2 is given as [25]:

$$E^{vdW} = -\frac{A_H}{12\pi} \left[\frac{1}{h^2} + \frac{1}{(h + \delta_1 + \delta_2)^2} - \frac{1}{(h + \delta_1)^2} - \frac{1}{(h + \delta_2)^2} \right] \quad (1)$$

where A_H is the combined Hamaker constant of the two surfaces interacting in the suspending medium, h is the separation distance between two interacting particles. At the closest approach, h was taken as 20 Å in all calculations for comparison with existing literature [7]. In the case of kaolinite, we have to consider six different surfaces for particle interaction, edge–edge, edge–silica face, edge–alumina face, silica–silica face, alumina–alumina face and silica face–alumina face interactions. Therefore, the non-retarded Hamaker constants for each of the six cases were determined from the Hamaker constant of silica and alumina as given in Table 1. Hamaker constants in the Table 1 were calculated from the following equation:

$$A_{123} = (\sqrt{A_{11}} - \sqrt{A_{33}})(\sqrt{A_{22}} - \sqrt{A_{33}}) \quad (2)$$

where A_{11} is the Hamaker constant for the first interacting surface, for example the silica face, alumina face or edge surface, A_{22} is the Hamaker constant for the second interacting surface, for example the silica face, alumina face or edge surface, and A_{33} = Hamaker constant for the suspending medium which in our study is water. The Hamaker constants for silica and alumina were taken as 8.86×10^{-20} J and 1.52×10^{-19} J, respectively [26]. The Hamaker constant for the edge surface was determined as 1.20×10^{-19} J from the average of the Hamaker constants for silica and alumina. The Hamaker constant for water was taken as 3.70×10^{-20} J [26].

Table 1: Hamaker constant of different interactions between kaolinite particles

Interaction	Interaction Type	Hamaker Constant, J
1	Edge–Edge	2.37×10^{-20}
2	Edge–Silica Face	1.63×10^{-20}
3	Edge–Alumina Face	3.05×10^{-20}
4	Silica Face–Silica Face	1.11×10^{-20}
5	Alumina Face–Alumina Face	3.90×10^{-20}
6	Silica Face–Alumina Face	2.08×10^{-20}

The electrical double layer interaction energy per unit area (E^{Edl}) between two planar surfaces with surface potentials ψ_1 and ψ_2 is given by the Hogg-Healy-Fuerstenau (HHF) expression for dissimilarly charged surfaces as [27]:

$$E^{Edl} = \varepsilon \varepsilon_0 \kappa \left[\frac{2\psi_1\psi_2 \exp(\kappa h) - \psi_1^2 - \psi_2^2}{\exp(2\kappa h) - 1} \right] \quad (3)$$

where ε_o is the permittivity of free space, ε is the dielectric constant and κ^{-1} is the Debye screening length of the electrical double layer.

For cases when the surface potential of the two planar surface are similar, i.e., $\psi_1 = \psi_2 = \psi$, the electrical double layer interaction energy reduces to

$$E^{Edl} = \frac{2\psi^2 \epsilon \kappa}{\exp(\kappa h) + 1} \quad (4)$$

Similarly, the electrical double layer interaction energy under the condition of constant surface charge, first established by Langmuir [28], can be used. In this case, revising equation (3) by replacing the two minus signs in the numerator by plus signs gives the Langmuir equation. In particular, the double layer interaction energy at constant surface potential and/or constant surface charge presents the lower and upper limits of the interaction energy. The actual double layer interaction energy with a mixed boundary condition or a surface charge regulation is between the two limits. The calculation shows that the trend of the total interaction energy for the cases is similar. Therefore, only the interaction energy described by equation (3) is used hereafter.

The resulting DLVO interaction energy is given as:

$$E = E^{vdW} + E^{Edl} \quad (5)$$

The total interaction energy was multiplied by the measured interaction area ratio of basal plane surface to edge surface of 13.39:1 as determined by atomic force microscopy. In calculating the

edge and face surface areas, the kaolinite particle was assumed to be a circular disc. The energies are scaled against the maximum predicted silica face-alumina face interaction energy, E_{max} .

Results and Discussion

The rheological behavior of a suspension is essentially determined by the forces that control the spatial arrangement and dynamics of the suspended particles. In a suspension under the predominant influence of repulsive electrostatic energies the particles tend to take up positions as far from each other as possible. This may lead to a regular arrangement of the particles, i.e., to the development of the spatial order in the suspension. Clusters of particles, or aggregate structures, form in a suspension when the particle interactions are dominated by attractive energies. The aggregate structure or flocs will immobilize the suspending medium, and give rise to increasing viscosity and yield strength of the suspension. The particle characteristics such as morphology, size, surface area, etc. will also greatly affect the suspension viscosity, and the strength of the aggregate structure. The aggregate structure plays a major part in the flow behavior of clay suspensions. The rate and mechanism of formation of such aggregate structures and the characteristics of the aggregate structures are therefore important parameters to describe the rheological characteristics of such suspensions. In this study, we will discuss the formation of aggregate structures of kaolinite and their validation by cryo-SEM in the following and subsequent sections.

Particle Interactions

As mentioned previously, the surface chemistry and rheology of kaolinite particles is complicated greatly by the non-uniform surface charge densities on edge and face surfaces. It was realized that electrophoretic measurements of kaolinite particles do not give detailed information about surface charge characteristics, and therefore information on electrophoretic mobility is not used in this analysis [29]. Instead, surface charge densities of the two faces of kaolinite particles (silica face and alumina face) were determined from surface force measurements are used in this analysis [12]. Recently Gupta *et al.* [13] used the zeta-potential for the edge surfaces as a linear combination of the zeta-potential of silica and alumina particles. It was realized that the zeta-potential does not define the surface potential of the edge surface appropriately. Instead, potentiometric titration was used to determine the surface potential and surface charge of the edge surface of kaolinite. The surface charge density for the edge surface of kaolinite was calculated from the following the charge balance as:

$$\sigma_{\text{kaolinite}} A_{\text{kaolinite}} = \sigma_{\text{silica face}} A_{\text{silica face}} + \sigma_{\text{alumina face}} A_{\text{alumina face}} + \sigma_{\text{edge face}} A_{\text{edge face}} \quad (6)$$

where $\sigma_{\text{kaolinite}}$ is the surface charge density of kaolinite particles as determined by potentiometric titration, $\sigma_{\text{silica face}}$ and $\sigma_{\text{alumina face}}$ are the surface charge densities of the silica face and the alumina face of kaolinite as determined by surface force measurements. The symbols $A_{\text{kaolinite}}$, $A_{\text{silica face}}$, $A_{\text{alumina face}}$ and $A_{\text{edge face}}$ represent the total area of kaolinite particles, area of silica face, alumina face and edge surfaces, respectively. The area of the silica face surface, the alumina face surface and the edge surface was determined from the kaolinite particle equivalent circle diameter and thickness, the details of which are provided in the Supporting Information.

With this information the surface charge densities of the edge surface of kaolinite was determined, and the results are presented in figure 2. As shown in figure 2, the surface charge density of the edge surface is significantly greater, over one order of magnitude greater when compared to the surface charge densities of the silica face and the alumina face of the kaolinite particles at high pH. At low pH, the surface charge density of the edge face of kaolinite is of a similar magnitude (within a factor of two) with that of the surface charge densities of the silica face and the alumina face.

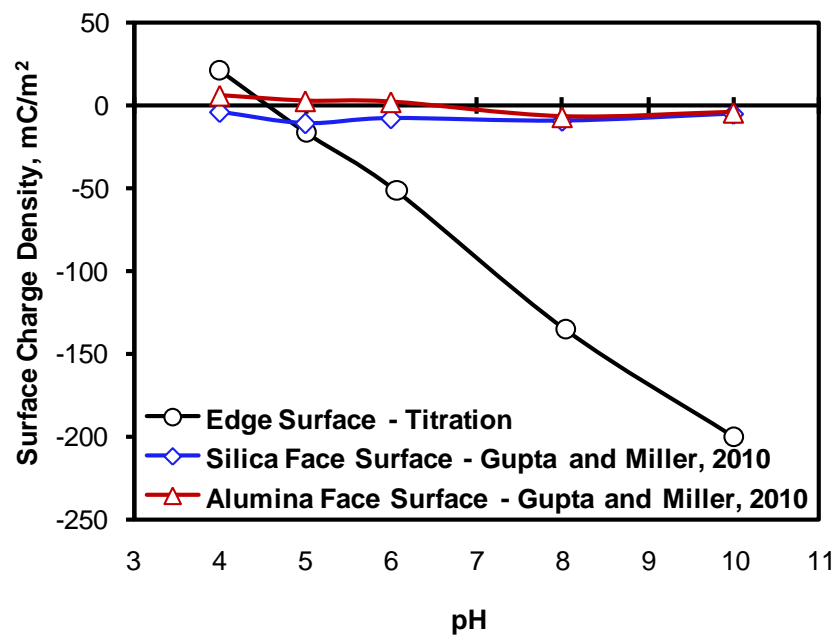


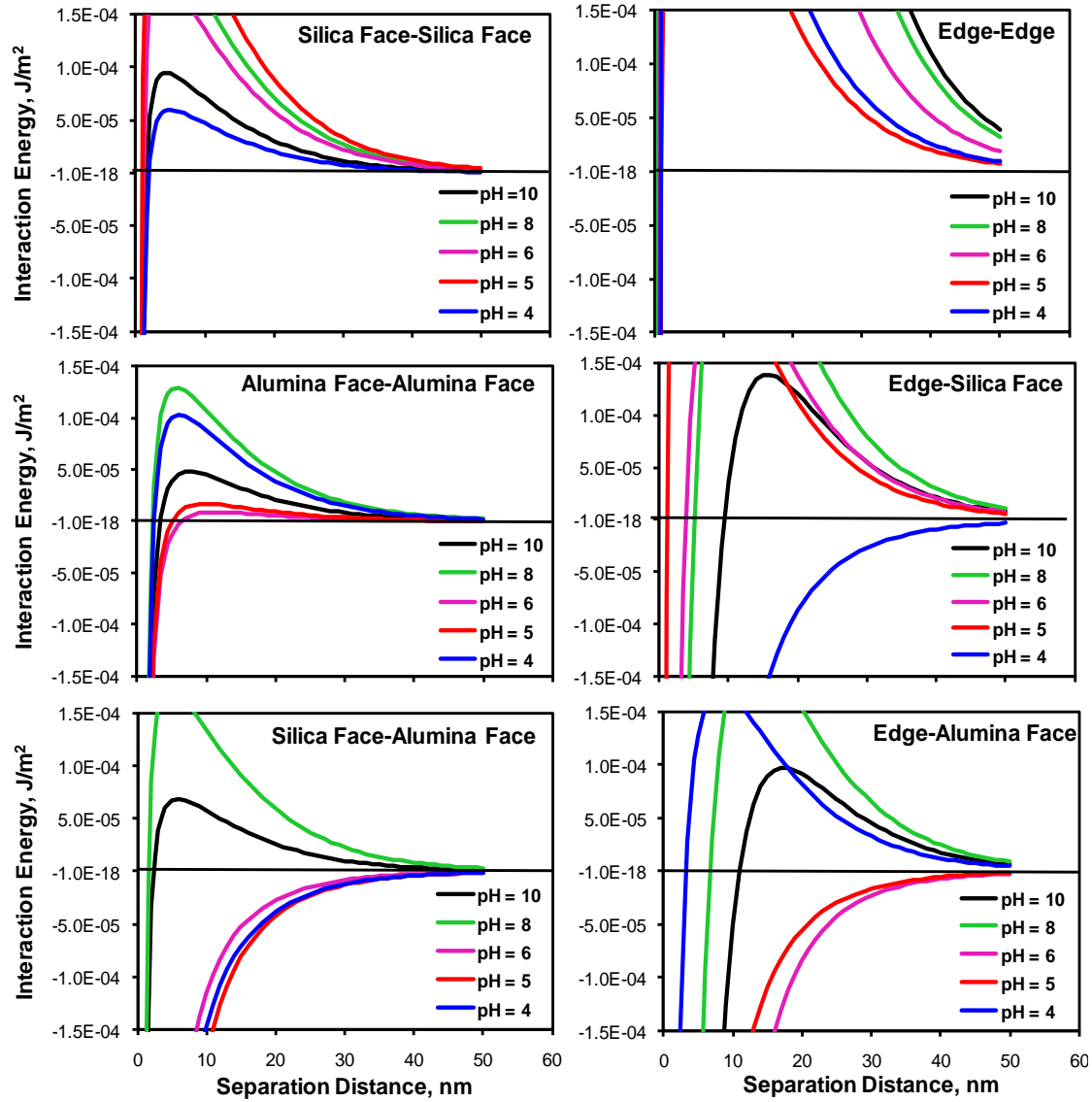
Figure 2: The surface charge densities of the kaolinite edge surface and the two face surfaces (silica and alumina face) as a function of pH in 1 mM KCl solution.

Considering the surface charge data provided for the different faces of kaolinite, the net interaction energy between different surfaces of kaolinite was determined and is shown in figure 3. The interaction energies were scaled to maximum attractive interaction energy determined for silica face–alumina face, and multiplied by the average interaction area ratio of 13.39:1 [13].

Figure 4 shows the scaled interaction energies calculated for a separation distance, $h = 20 \text{ \AA}$, when there is no energy barrier, consistent with previous studies [7]. When there is an energy barrier between surface interactions, the interaction energies were calculated at the separation distance for the maximum energy barrier.

It is evident that the silica face–silica face interaction is repulsive in the pH range of 4–10 due to the strong electrostatic repulsion between negatively charged silica faces (see Figure 3 and Figure 4). The alumina face–alumina face interactions showed a slight repulsion with a small energy barrier at pH 6 due to weak electrostatic repulsion and stronger van der Waals attraction. Below pH 7.5, the silica face–alumina face interaction is attractive with a maximum at pH 5, whereas a slight repulsion was observed at higher pH ($\text{pH} > 7.5$). This is due to the opposite sign of the surface charge densities for the silica face and alumina face at $\text{pH} \leq 6$ (silica face is negatively charged and alumina face is positively charged), causing stronger attraction both electrostatic and van der Waals attraction (see Figure 3 and Figure 4). At higher pH ($\text{pH} \geq 8$), both the silica face and alumina face carry the same surface charge sign (both silica and alumina face carry negative charge), and hence a slight repulsive electrostatic interaction was found. The edge–edge surfaces showed repulsive interaction for the entire pH range, due to the similar nature of surface charge, i.e., edge surfaces carry a positive surface charge at pH 4, which

becomes increasingly negative at pH values greater than 5 (see Figure 2). The edge–alumina face showed repulsive interactions at low pH (pH of 4) and at high pH ($\text{pH} \geq 8$) due to strong electrostatic repulsive interactions, whereas an attractive interaction was found at an intermediate pH of 5–6. In contrast, the edge–silica face showed attractive interaction only at low pH 4 and repulsion at a higher pH ($\text{pH} \geq 5$), due to similar nature of the surface charge on the edge surface and the silica face of kaolinite at higher pH. The edge–silica face and edge–alumina face interactions indicate that the edge–face interactions are favorable at $\text{pH} < 8$. Though the magnitude of edge–silica face and edge–alumina face interactions suggest an insignificant interaction on an interaction area basis, the interaction cannot be ignored as the edge effect could become significant in concentrated suspensions when the kaolinite particles are stacked due to the silica face–alumina face interaction.



1
2 Figure 3: Interaction energy profiles for different surface interactions of kaolinite particles.

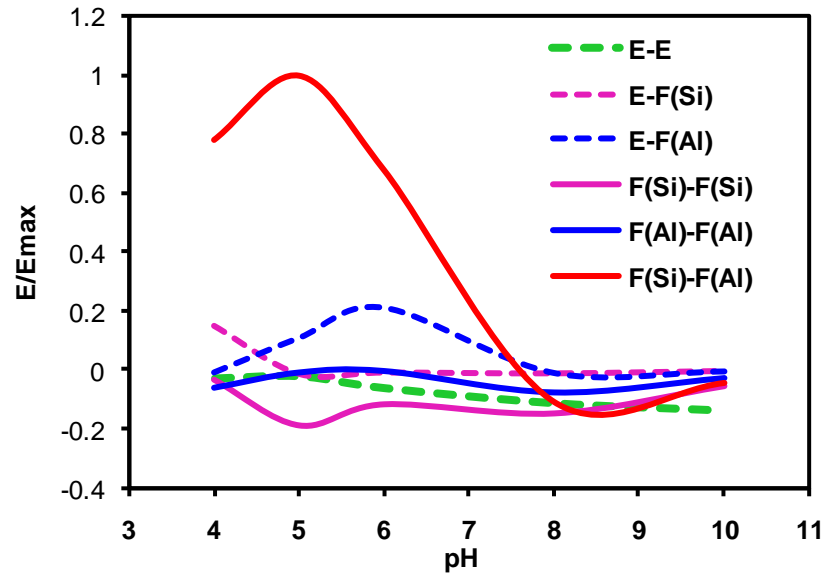


Figure 4: The predicted kaolinite edge–edge, edge–silica face (E-F(Si)), edge–alumina face (E-F(Al)), silica face–silica face (F(Si)-F(Si)), alumina face–alumina face (F(Al)-F(Al)), and silica face–alumina face (F(Si)-F(Al)) interaction energies scaled to maximum attractive energy for the silica face–alumina face interaction. Kaolinite particles with diameter 600 nm and thickness 11.2 nm in 1 mM KCl solution.

On the basis of these different interactions shown in Figure 3 and Figure 4, it is expected that the overall interaction of kaolinite particles will be dominated by silica face–alumina face in acidic solutions ($\text{pH} < 7.5$). Whereas, the alumina face–alumina face interactions are unfavorable over the entire pH range of the system. Although lower in magnitude, the edge–silica face showed favorable interaction at low pH of 4, and therefore some edge–face associations will also be expected at low pH. It is therefore anticipated that the kaolinite particles will aggregate initially in a silica face–alumina face manner forming a lamellar tactoid structure in kaolin suspensions at low pH values [5]. This results in a lower suspension shear yield stress. As the pH rises, the

face–face association will grow, causing the formation of tactoids with thicker edge surfaces, and thereby promoting the edge–face association. This is supported by Secor and Radke [30] who found by numerical simulation that the electrostatic field from the basal plane may “spill-over” to dominate the positive edge surface. Chang and Sposito [31] also showed that the negative electric field from the basal plane of a disc-shaped clay mineral particle near the edge surface is mainly controlled by particle thickness. This face–face association is found to be dominant at pH 5, and edge–face associations dominant at pH 6, which corresponds to the maximum shear yield stress at pH 5-5.5. As the pH is increased further, the face–face and edge–face association decreases due to lower magnitude of surface charge density on edge surfaces and face surfaces resulting in lower shear yield stress. At high pH, the edge–face and face–face interaction forces become repulsive, and the system becomes completely dispersed, and a negligible shear yield stress is measured. In this way, the maximum shear yield stress at pH 5.5 can be explained based on particle aggregation and its variation with system pH. Even if the edge surface charge density and corresponding interactions are based on zeta potential measurements as dismissed at the beginning of this section on particle interactions, the relative significance of some interactions changes but in general the same conclusion is found regarding the variation of interactions with pH.

O’Brien [15] observed the dominant face-face and some face-edge aggregation behavior of kaolinite both in distilled water and in electrolyte solutions using scanning electron microscopy of freeze-dried kaolinite samples. However, concern was raised that the freeze-drying technique can alter the structure of these aggregates during drying. Recently, Zbik *et al.* [22] observed stacks of kaolinite aggregated dominantly in face-face manner at pH 8 using cryo-vitrified

technique with scanning electron microscopy. The authors could not explain the face–face type interaction based on the assumption that 001 and 00 $\bar{1}$ faces of kaolinite are negatively charged. Instead, it follows from our new results that the kaolinite particles are aggregating according to silica face–alumina face and alumina face–alumina face interactions.

In contrast to our results, Johnson *et al.* [7, 8] predicted that the kaolinite particles will mostly interact in an edge–face manner at lower pH. However, their studies were based on the assumption that both faces of kaolinite are negatively charged, which analysis must be reconsidered in view of the AFM surface force results reported by Gupta and Miller [12]. These different surface interactions are of importance in order to control the aggregation behavior of kaolinite particles, and the mechanical properties of such suspensions.

Influence of Aspect Ratio

The influence of aspect ratio (ratio of particle diameter to thickness) on the different surface interactions is shown in figure 5. The aspect ratio was determined from the atomic force microscopy images of kaolinite particles. About 150 particles were imaged and analyzed using Nanoscope V7.2 software for the atomic force microscope (Veeco Instruments Inc., Santa Barbara, CA). As shown, the edge–silica face and edge–alumina face interactions are significant for particles with a low aspect ratio (9) as compared to particles with a high aspect ratio (165). Notably, the edge–alumina face interactions are dominant at pH 6, whereas silica face–alumina face interactions are dominant at pH 5 for kaolinite particles with low aspect ratio. This is particularly interesting as significant edge–face interaction for particles with a low aspect ratio

indicates that particles will orient themselves in both edge–face and face–face (silica face–alumina face) organizations. The particles with high aspect ratio will orient themselves dominantly in a face–face manner (silica face–alumina face). It is shown that the aggregate structures can be expected to depend on the aspect ratio of kaolinite particles, and thereby the mechanical properties of the kaolinite suspensions will be affected by the aspect ratio.

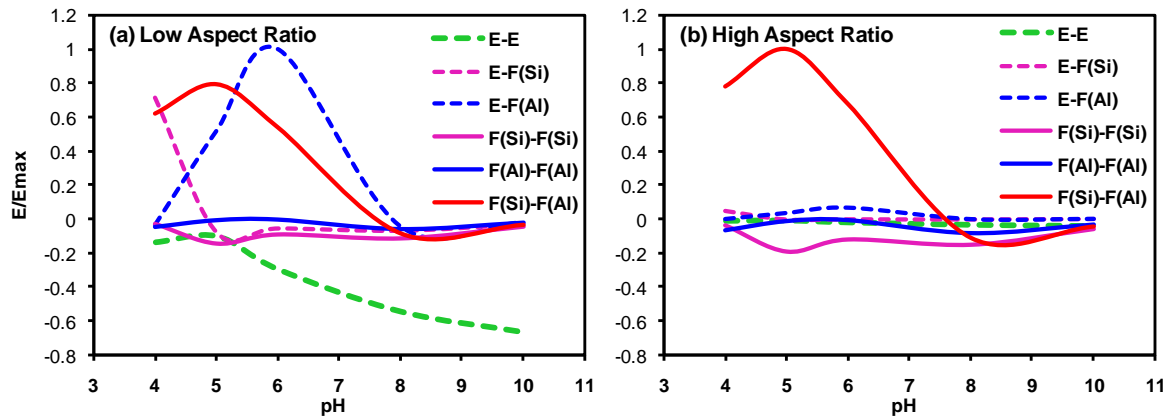


Figure 5: Effect of aspect ratio on different face type interaction of kaolinite particles (a) low aspect ratio = 9 and (b) high aspect ratio = 165 in 1 mM KCl solution. The symbols E, F(Si) and F(Al) represent edge, silica face, and alumina face, respectively.

Influence of Electrical Double Layer Thickness

Figure 6 shows the effect of electric double layer thickness on the different surface interactions. Particles suspended at high ionic strength will experience a small double layer thickness (3.04 nm) (see Figure 6b). Under these circumstances there is a greater alumina face–alumina face

attraction and greater repulsion of silica faces, and edge faces when compared to particles suspended in a solution with a larger double layer thickness (9.6 nm) (see Figure 6a). Also at high ionic strength, there is a greater increase in the edge–alumina face interactions which promote edge–face associations as compared to low ionic strength. It is evident that at high ionic strength, i.e., at small values of the reciprocal of the Debye constant (the thickness of the double layer), $\kappa^{-1} = 3.04$ nm, the silica face–alumina face interactions will be increased at pH 5 with improved aggregation. At the same time, the increased alumina face–alumina face interactions will expose the silica faces on the kaolinite particles, which may also further promote aggregation with alumina faces, forming a larger aggregate structure. Olphen [17] observed decreasing viscosity and yield stress of dilute and concentrated clay suspensions at lower NaCl concentration. With further addition of NaCl, both the viscosity and the yield stress increase, slowly at first, and rather sharply when the flocculating concentration of NaCl for the clay was approached.

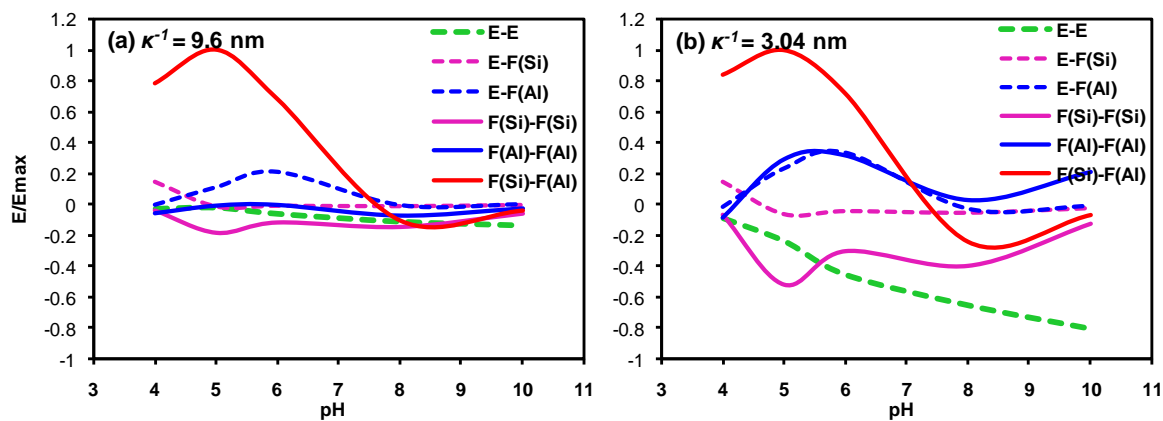


Figure 6: Effect of electric double layer thickness (κ^{-1}) on different surface interactions for kaolinite particles with particle diameter 600 nm and thickness 11.2 nm at (a) $\kappa^{-1} = 9.6$ nm (1

mM KCl solution) and (b) $\kappa^{-1} = 3.04$ nm (10 mM KCl solution). The zeta-potentials of the silica face and the alumina face are assumed to be reduced by 30% with increasing ionic strength from 1 mM to 10 mM KCl solution. The edge surface potential data for 10 mM KCl solution were taken from literature [14]. The symbols E, F(Si) and F(Al) represent edge, silica face, and alumina face surfaces, respectively.

Aggregate Structure

In a suspension of clay particles, three different modes of particle association or aggregate structure may occur: face–face, edge–face, and edge–edge [17]. The DLVO interaction energies (electrostatic energy and the van der Waals interaction energy) for the three types of association are governed by six different combinations of the three surfaces interactions – the silica face, the alumina face and the edge surface, as explained previously. Consequently, the three types of association will not necessarily occur simultaneously or to the same extent when a kaolinite suspension is aggregated.

Face–face associations will lead to thicker and possibly larger aggregates, whereas edge–face and edge–edge associations will form three-dimensional voluminous card-house structures [17]. The various modes of particle association are shown in figure 7.

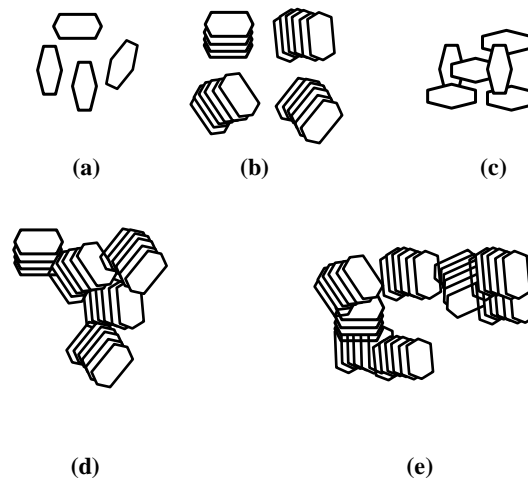


Figure 7: The formation of aggregate structures in kaolinite suspensions, as (a) dispersed, (b) face-face, (c) edge-face, (d) edge-edge, and (e) a combination of (b), (c) and (d), depending on the solution chemistry of the suspension.

The SEM micrographs of kaolinite aggregates under cryogenic conditions at pH 3, 5, 7, and 9 are shown in figure 8. It can be seen that the kaolinite particles are mostly associated in a face-face manner (silica face-alumina face and/or alumina face-alumina face), and some face-edge organization (edge-silica face) at pH 3 and pH 5 (see Figure 8). This is in good agreement with the theoretical predictions that at low pH, the attraction between the silica face and the alumina face dominates and thereby accounts for the face-face association. This face-face association also promotes edge-face aggregation of kaolinite particles with an increase in pH to pH 5.

At pH 7, the particles are mostly associated in edge-edge manner and edge-face manner (edge-silica face) (Figure 8). At higher pH (pH = 9), the particles are mostly associated in edge-edge manner creating a porous structure. Also, due to repulsion between the silica face and alumina

face, face–face association was not observed at pH 9, in agreement with theoretical considerations. The edge–edge interaction at pH 9.0 should also be unfavorable due to similar surface charge density at the edge surfaces, which causes repulsion. The edge–edge associations at high pH 9 were contrary to DLVO expectation, since all the surfaces of kaolinite particles are negatively charged, and the suspension is stable. In agreement with our observation, Zbik and Horn [32] also observed similar structures involving edge–edge association for kaolinite particles, and they proposed that hydrophobic interaction between edge surfaces could contribute to such structures. Such a proposition needs further consideration. Alternatively, the edge–edge association observed at pH 9.0 may be due to the experimental conditions associated with freezing the sample under cryogenic conditions.

The cryogenic-SEM images showed the kaolinite aggregate structure for a 4% kaolinite suspension. This concentration may well be above the gelation point [23], but the general trends of the aggregate structure showing dominant face-face association was also observed in dilute (0.01%) and semi-dilute (0.1%) kaolinite suspensions (SEM graphs not shown). Our results are also supported by Zbik and Frost [23] who observed similar face–face and edge–face contacts in kaolinite from Georgia. Other modes of particle associations such as stair step edge–edge contacts were also revealed in Birdwood kaolinite aggregates [23].

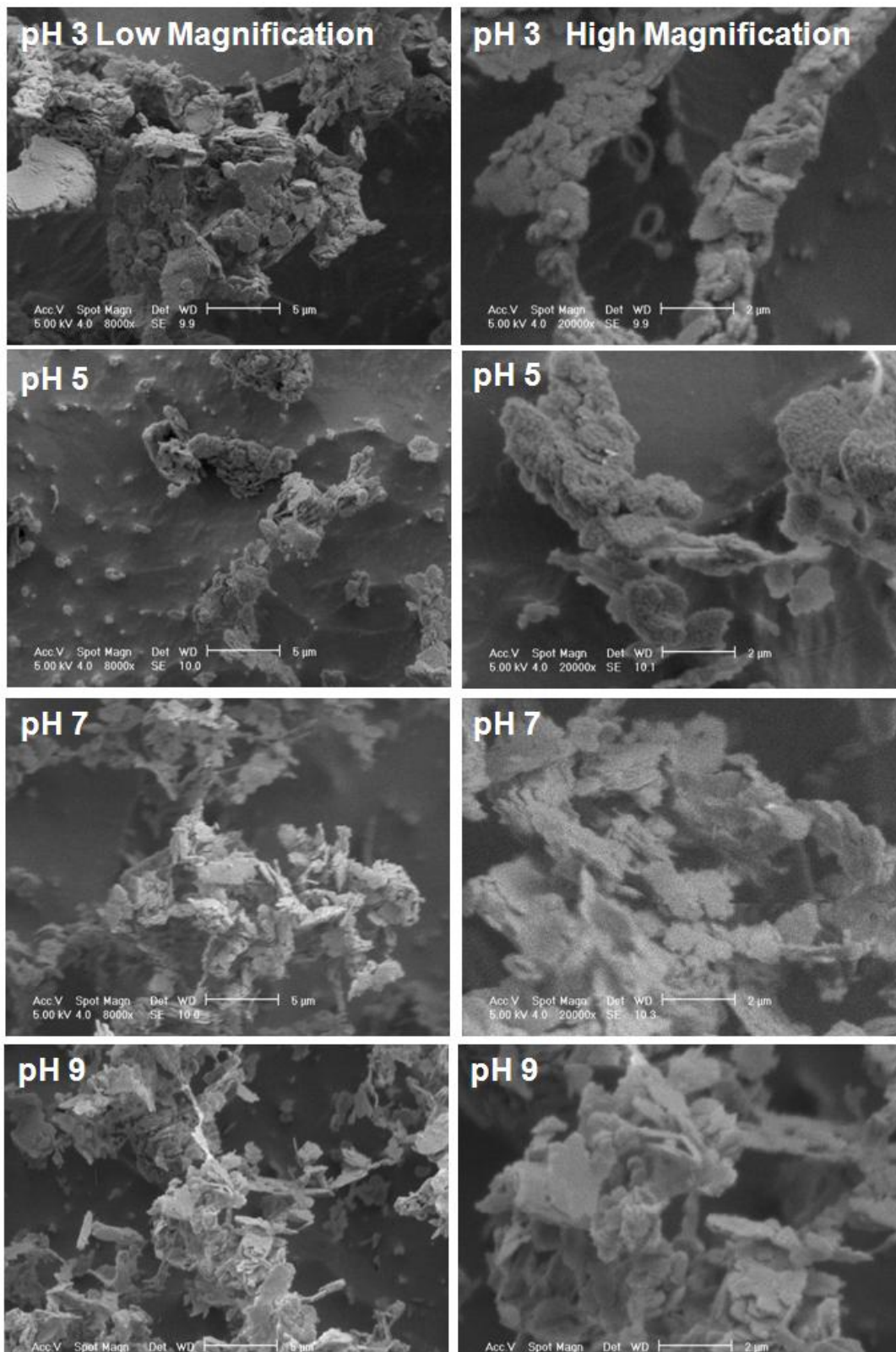


Figure 8: Cryo-SEM micrographs of kaolinite aggregates at pH 3, 5, 7 and 9 at low (left) and high (right) magnification.

Aggregate Size

The aggregate structure of kaolinite suspensions at different pH values as revealed by cryo-SEM are also supported by further experiments conducted using photon correlation spectroscopy (PCS) to estimate the particle size of such aggregates. In our analysis, we estimated the equivalent sphere diameter of aggregate-structures for kaolinite suspensions. These aggregate structures for kaolinite suspensions are three dimensional networks of particles forming an arbitrary shape or so called “card-house” structure [17]. The precise information for the size of aggregate structures in kaolinite suspensions could not be revealed with present instrumentation, and only qualitative trends are realized. Figure 9 shows the average particle size of kaolinite aggregates in suspension as a function of pH. As shown, the average aggregate size of kaolinite is about 16.3 ± 0.3 nm at pH 7 and 9. The average aggregate size of kaolinite remains unchanged when measured as a function of time at pH 9, which represents a more dispersed state for the kaolinite particles. The aggregate size grows to 38.9 ± 0.3 nm at pH 7 in 40 minutes, which could be indicative of a loose aggregate structure formed mainly by edge–edge associations. The initial aggregate size for kaolinite suspensions at pH 3.5 and 5 were 266.8 ± 12.0 nm and 127.1 ± 7.9 nm, respectively. The aggregates of kaolinite grow over an order of magnitude in size in just a few minutes at pH 3 and 5, and then remain constant. These results suggest that kaolinite particles are associated with all three modes of interactions – face–face, edge–face and edge–edge – forming a

three-dimensional network. These results were also supported by fractal dimension of kaolinite aggregate structure determined by MasterSizer 2000E, which indicates that the shape of the kaolinite aggregates at low pH of 3 and 5 is close to the shape of one-dimensional objects. At high pH the fractal dimension increases to 2, which implies that the shape of the aggregates at high pH resembles the shape of two-dimensional objects (see Supporting Information). Of course, as stated previously, the aggregate structure as revealed by cryo-SEM and PCS will influence the mechanical properties of kaolinite suspensions, and thereby affect the rheological properties of such suspensions.

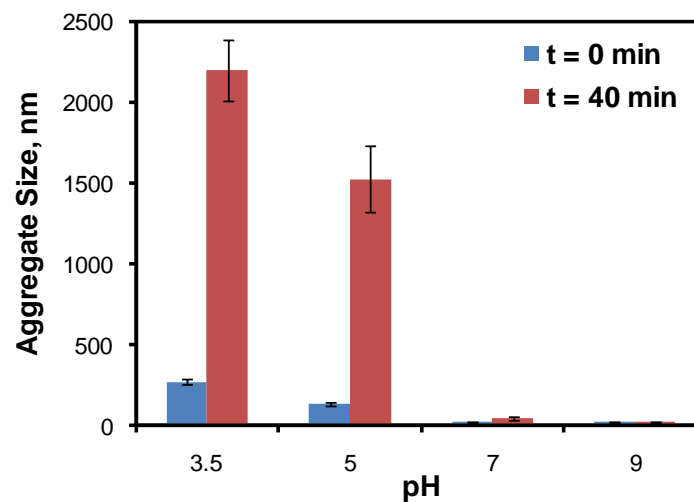


Figure 9: Average aggregate size for a suspension of kaolinite particles as a function of pH.

Conclusion

1 The mechanical properties of kaolinite suspensions particularly the shear yield stress is explained
2 based on the aggregate structure of the kaolinite particles. A new analysis based on the surface
3 charge densities of the silica face, alumina face and edge surfaces demonstrate the role of pair-
4 wise interactions in controlling the rheology of kaolinite particulate suspensions. The maximum
5 shear yield stress of kaolinite suspensions is indicative of the significant role played by particle
6 organization in the formation of aggregates as governed by edge–edge, edge–silica face, edge–
7 alumina face, silica face–alumina face, silica face–silica face, and alumina face–alumina face
8 interaction energies.

9
10 The results indicate that the face–face (silica face–alumina face) is the dominant particle
11 interaction at low pH values, which promotes edge–face (edge–silica face and edge–alumina
12 face) and face–face (silica face–alumina face) interaction at intermediate pH values, justifying
13 the maximum shear yield stress at pH 5-5.5. This conclusion is also confirmed by cryo-SEM
14 analysis of kaolinite aggregate structure and photon correlation spectroscopy. At a higher pH (pH
15 = 7), the kaolinite aggregates show edge–edge and edge–face interactions, whereas a more
16 porous structure of aggregates was observed at high pH (pH = 9).

17
18 The influences of particle aspect ratio and electrical double layer thickness were also examined
19 to determine their effect on interaction energies. The findings show that the edge surface–silica
20 face interactions become favorable at a low aspect ratio, whereas the silica face–alumina face
21 and alumina face–alumina face interactions are increased at high ionic strength conditions. These
22 different interactions and their relative significance, provide the basis for a more detailed

1 explanation of the rheological behavior of kaolinite suspensions as well as an improved
2 foundation for the modification of kaolinite interactions and control of rheological properties.

3 4 **Acknowledgement**

5
6 The authors wish to acknowledge the financial support of grant DE-FG-03-93-ER14315 from
7 DOE Basic Sciences and grant DP0663688 from the Australian Research Council, and the CMM
8 at the University of Queensland for the use of the cryogenic SEM.

9 10 **Supporting Information Available**

11
12 Details regarding particle size, thickness, aspect ratio, area of silica face surface, alumina face
13 surface and edge surface, and fractal dimension of kaolinite aggregates are provided.

14 15 **References**

- 16
17 [1] C.C. Harvey, H.H. Murray, *Applied Clay Science* 11 (1997) 285.
18 [2] H.H. Murray, *Applied Clay Science* 17 (2000) 207.
19 [3] F. Franco, L.A. Perez-Maqueda, J.L. Perez-Rodriguez, *Journal of Colloid and Interface*
20 *Science* 274 (2004) 107.
21 [4] N. Street, A.S. Buchanan, *Australian Journal of Chemistry* 9 (1956) 450.
22 [5] R.K. Schofield, H.R. Samson, *Discussions of the Faraday Society* 18 (1954) 135.
23 [6] N. Street, *Australian Journal of Chemistry* 9 (1956) 467.
24 [7] S.B. Johnson, A.S. Russell, P.J. Scales, *Colloids and Surfaces A: Physicochemical and*
25 *Engineering Aspects* 141 (1998) 119.
26 [8] S.B. Johnson, G.V. Franks, P.J. Scales, D.V. Boger, T.W. Healy, *International Journal of*
27 *Mineral Processing* 58 (2000) 267.
28 [9] B. Rand, I.E. Melton, *Journal of Colloid and Interface Science* 60 (1977) 308.
29 [10] I. Sondi, O. Milat, V. Pravdic, *Journal of Colloid and Interface Science* 189 (1997) 66.

- 1 [11] C. Chassagne, F. Mietta, J.C. Winterwerp, Journal of Colloid and Interface Science 336
- 2 (2009) 352.
- 3 [12] V. Gupta, J.D. Miller, Journal of Colloid and Interface Science 344 (2010) 362.
- 4 [13] V. Gupta, J.D. Miller, A.V. Nguyen, in: (Ed.)^(Eds.)Conference of Metallurgists;
- 5 MetSoc, Vancouver, BC, 2010.
- 6 [14] D.J.A. Williams, K.P. Williams, Journal of Colloid and Interface Science 65 (1978) 79.
- 7 [15] N.R. O'Brien, Clays and Clay Minerals, Proceedings of the Conference 19 (1971) 353.
- 8 [16] A. Casagrande, in: (Ed.) Boston Society of Civil Engineers, 1940, p 72.
- 9 [17] H.V. Olphen, An introduction to clay colloid chemistry : for clay technologists,
- 10 geologists and soil scientists. Interscience, New York, 1963.
- 11 [18] T.W. Lambe, in: (Ed.) American Society of Civil Engineers, 1953, p 1.
- 12 [19] T.K. Tan, in: (Ed.) 4th International Conference on Soil Mechanics and Foundation
- 13 Engineering Proceedings, 1958, p 87.
- 14 [20] I.T. Rosenqvist, in: (Ed.) Norwegian Geotechnical Institute; Norwegian Geotechnical
- 15 Institute, 1963, p 1.
- 16 [21] I.T. Rosenqvist, in: (Ed.) American Society of Civil Engineers Proceedings; American
- 17 Society of Civil Engineers, 1959, p 31.
- 18 [22] M.S. Zbik, R.S.C. Smart, G.E. Morris, Journal of Colloid and Interface Science 328
- 19 (2008) 73.
- 20 [23] M.S. Zbik, R.L. Frost, Journal of Colloid and Interface Science 339 (2009) 110.
- 21 [24] J.I. Bidwell, W.B. Jepson, G.L. Toms, Clay Minerals 8 (1970) 445.
- 22 [25] J.H. Masliyah, S. Bhattacharjee, Electrokinetic and Colloid Transport Phenomena. John
- 23 Wiley & Sons, Inc., 2006.
- 24 [26] L. Bergstrom, Advances in Colloid and Interface Science 70 (1997) 125.
- 25 [27] A.V. Nguyen, H.J. Schulze, Colloidal Science of Flotation. Marcel Dekker, Inc., 2004.
- 26 [28] I. Langmuir, Journal of Chemical Physics 6 (1938) 873.
- 27 [29] J.D. Miller, J. Nalaskowski, B. Abdul, H. Du, Canadian Journal of Chemical Engineering
- 28 85 (2007) 617.
- 29 [30] R.B. Secor, C.J. Radke, Journal of Colloid and Interface Science 103 (1985) 237.
- 30 [31] F.R.C. Chang, G. Sposito, Journal of Colloid and Interface Science 163 (1994) 19.
- 31 [32] M. Zbik, R.G. Horn, Colloids and Surfaces A: Physicochemical and Engineering Aspects
- 32 222 (2003) 323.
- 33

Table 2: Hamaker constant of different interactions between kaolinite particles

Interaction	Interaction Type	Hamaker Constant, J
1	Edge–Edge	2.37×10^{-20}
2	Edge–Silica Face	1.63×10^{-20}
3	Edge–Alumina Face	3.05×10^{-20}
4	Silica Face–Silica Face	1.11×10^{-20}
5	Alumina Face–Alumina Face	3.90×10^{-20}
6	Silica Face–Alumina Face	2.08×10^{-20}

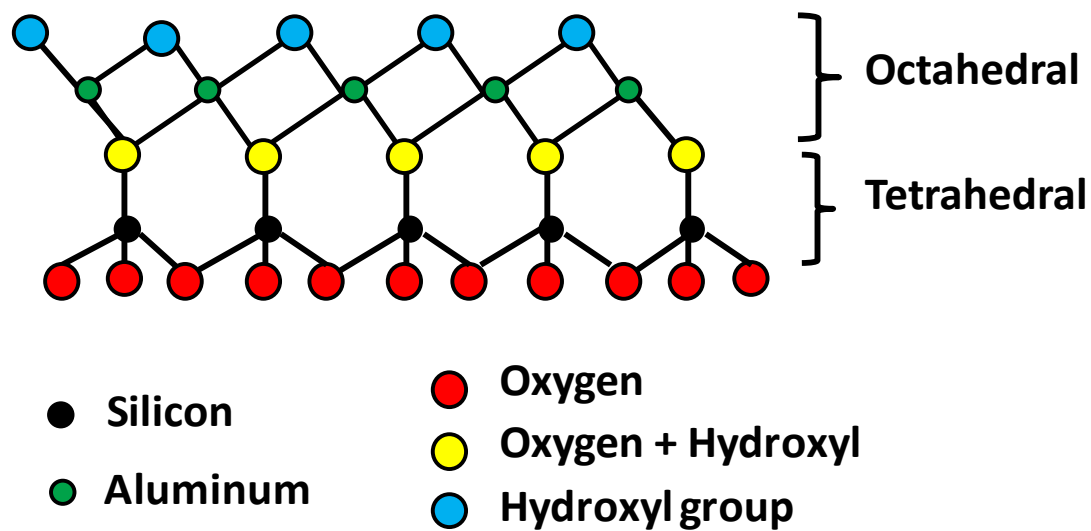


Figure 10: The structure of kaolinite along 010 edge surface showing a silica tetrahedral layer and an alumina octahedral layer.

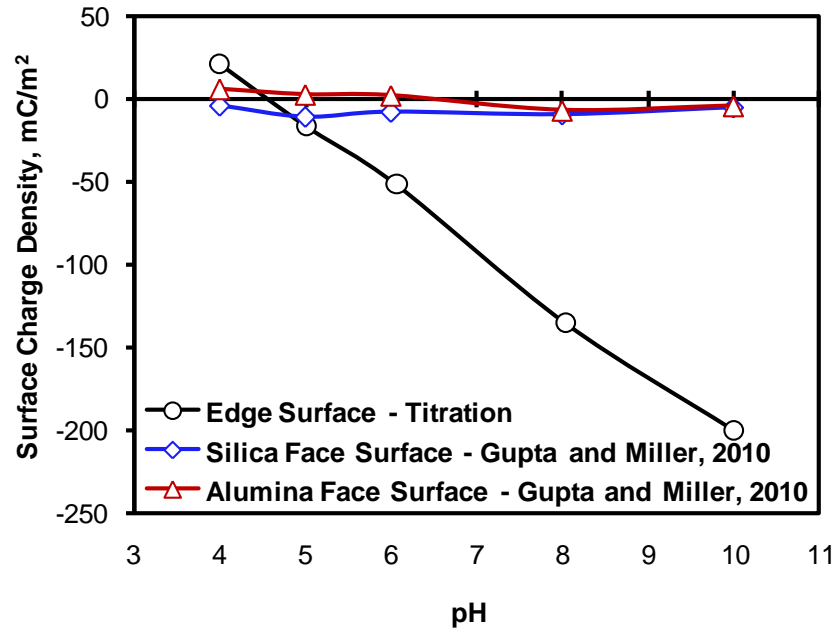


Figure 11: The surface charge densities of the kaolinite edge surface and the two face surfaces (silica and alumina face) as a function of pH in 1 mM KCl solution.

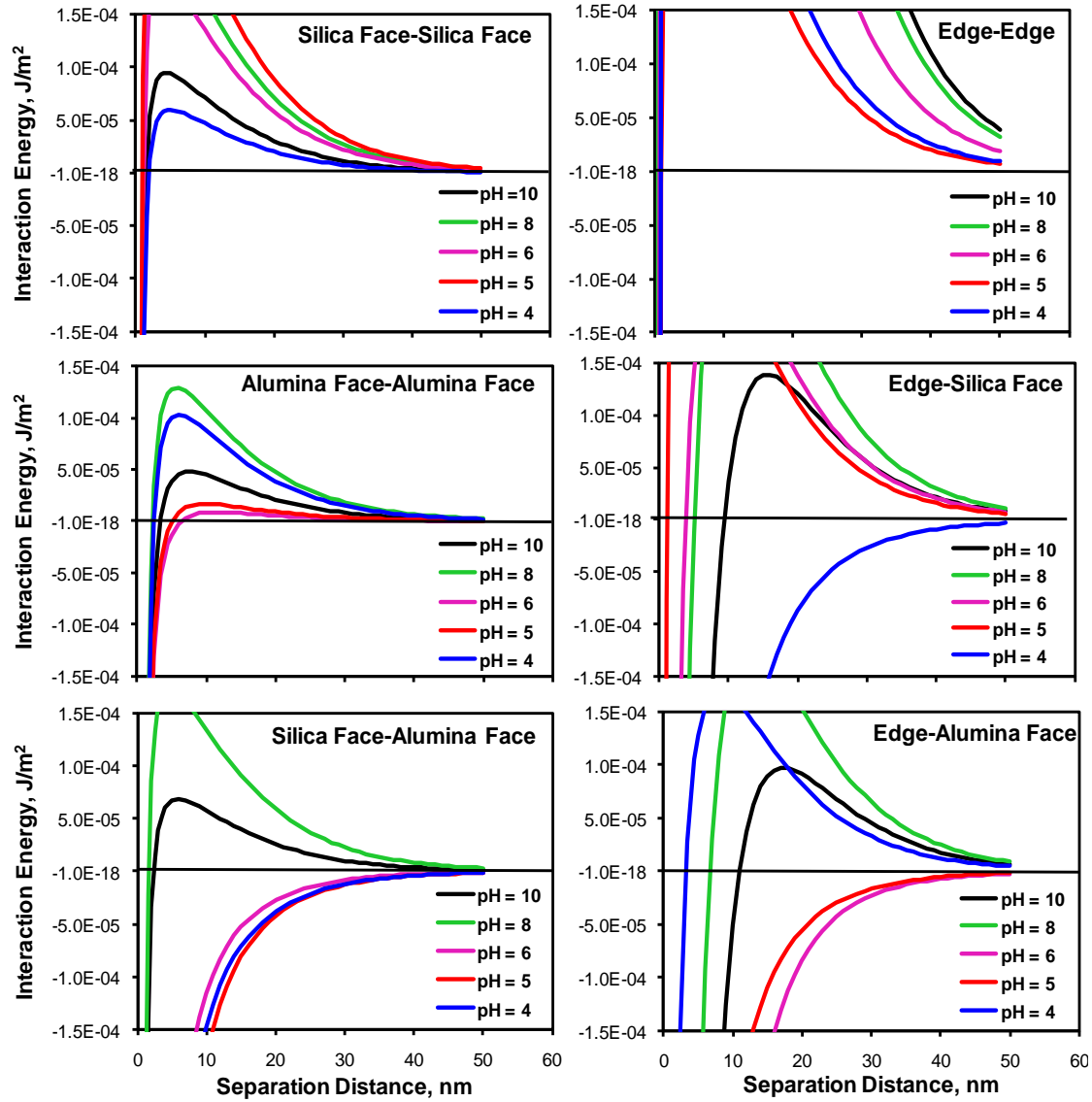


Figure 12: Interaction energy profiles for different surface interactions of kaolinite particles.

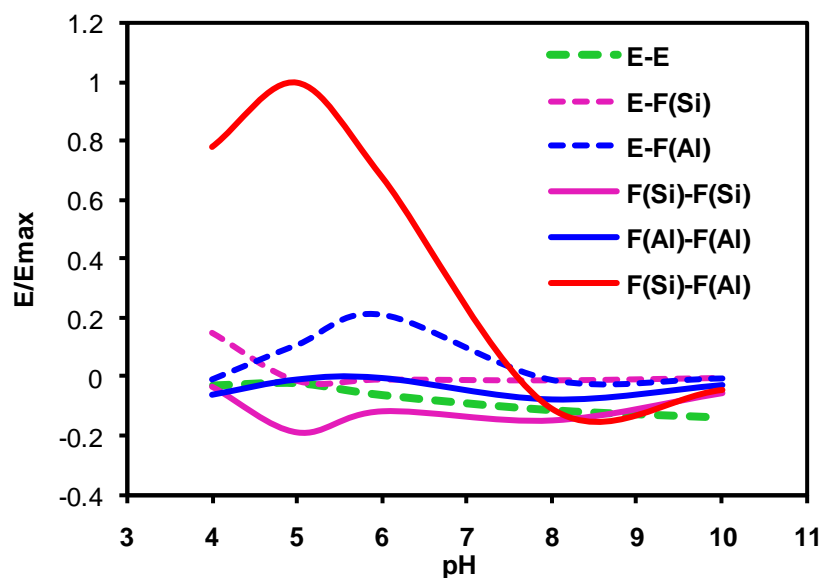


Figure 13: The predicted kaolinite edge–edge, edge–silica face (E-F(Si)), edge–alumina face (E-Al(Si)), silica face–silica face (F(Si)-F(Si)), alumina face–alumina face (F(Al)-F(Al)), and silica face–alumina face (F(Si)-F(Al)) interaction energies scaled to maximum attractive energy for the silica face–alumina face interaction. Kaolinite particles with diameter 600 nm and thickness 11.2 nm in 1 mM KCl solution.

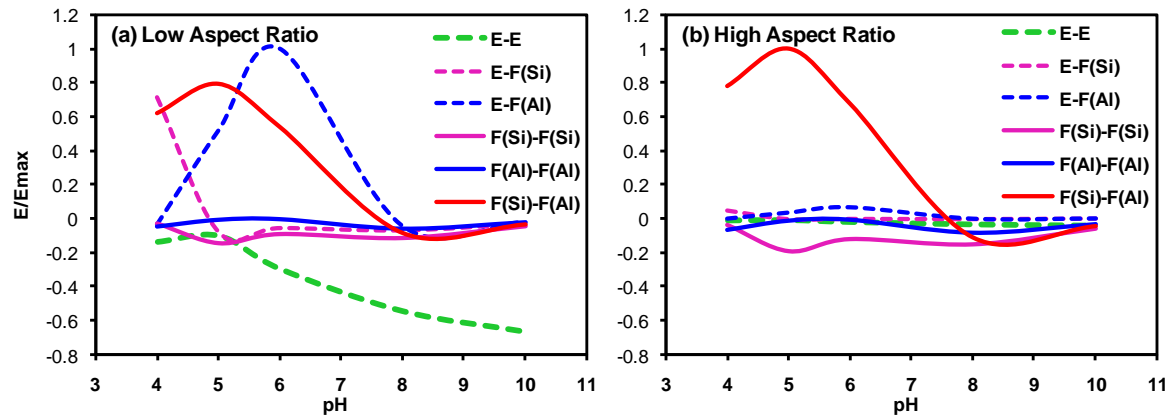


Figure 14: Effect of aspect ratio on different face type interaction of kaolinite particles (a) low aspect ratio = 9 and (b) high aspect ratio = 165 in 1 mM KCl solution. The symbols E, F(Si) and F(Al) represent edge, silica face, and alumina face, respectively.

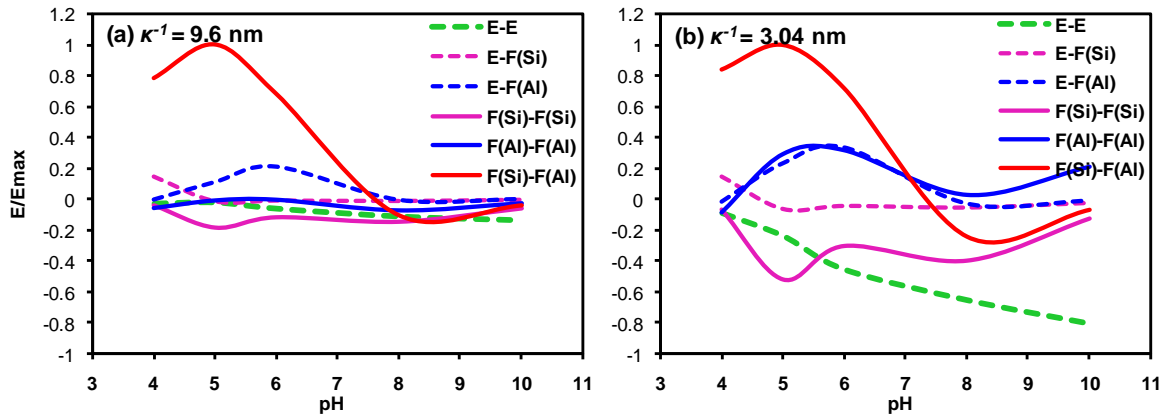


Figure 15: Effect of electric double layer thickness (κ^{-1}) on different surface interactions for kaolinite particles with particle diameter 600 nm and thickness 11.2 nm at (a) $\kappa^{-1} = 9.6$ nm (1 mM KCl solution) and (b) $\kappa^{-1} = 3.04$ nm (10 mM KCl solution). The zeta-potentials of the silica face and the alumina face are assumed to be reduced by 30% with increasing ionic strength from 1 mM to 10 mM KCl solution. The edge surface potential data for 10 mM KCl solution were taken from literature [14]. The symbols E, F(Si) and F(Al) represent edge, silica face, and alumina face surfaces, respectively.

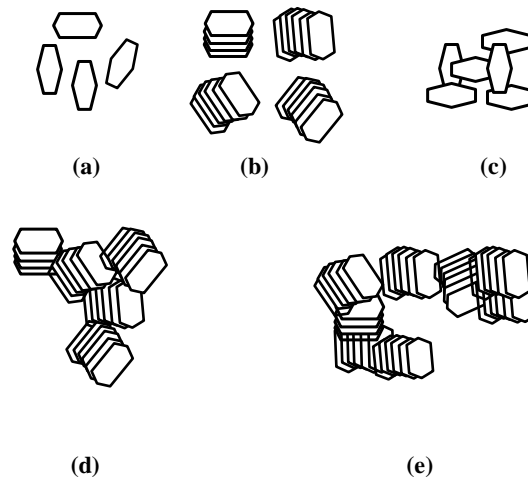


Figure 16: The formation of aggregate structures in kaolinite suspensions, as (a) dispersed, (b) face–face, (c) edge–face, (d) edge–edge, and (e) a combination of (b), (c) and (d), depending on the solution chemistry of the suspension.

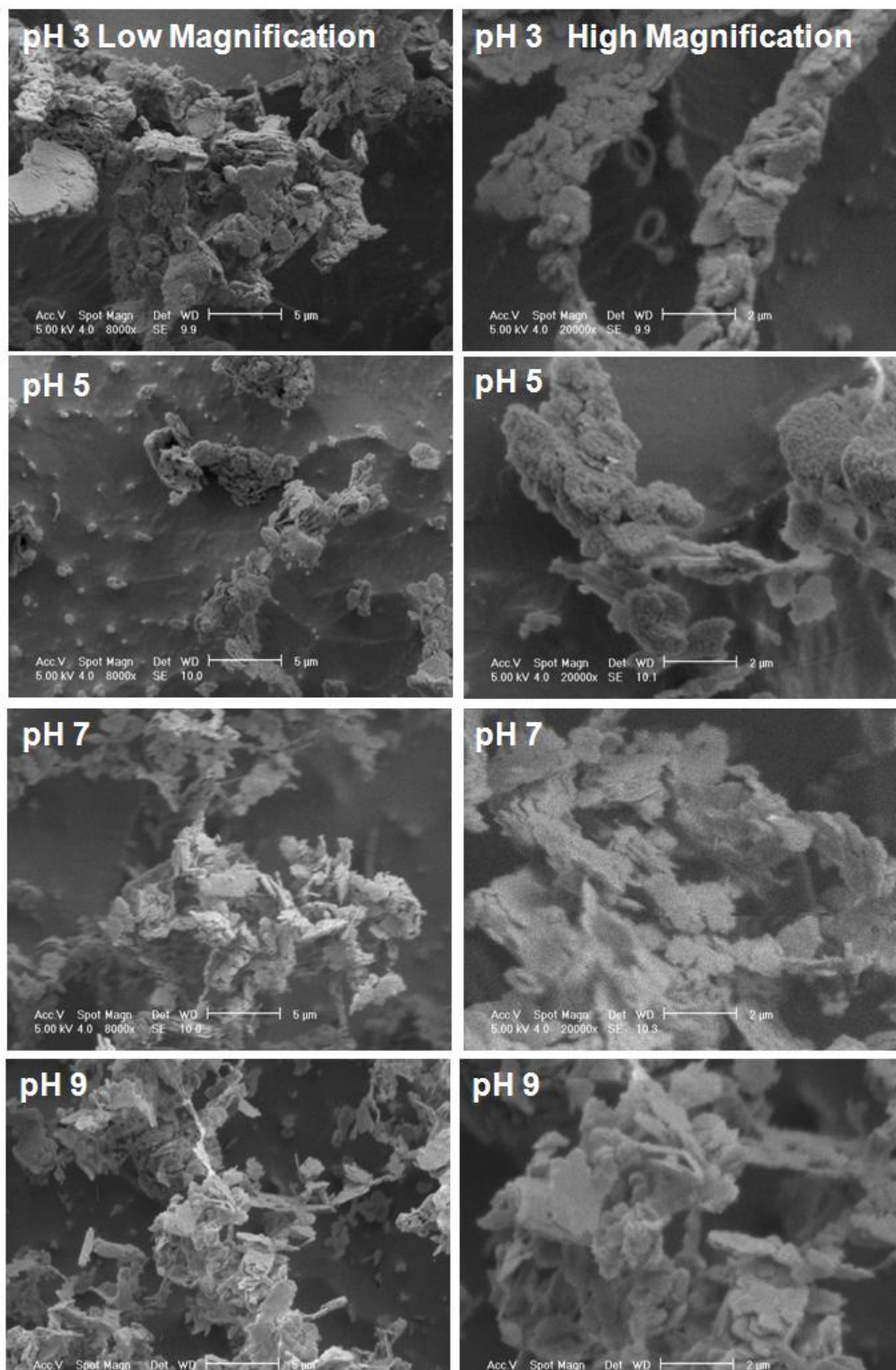


Figure 17: Cryo-SEM micrographs of kaolinite aggregates at pH 3, 5, 7 and 9 at low (left) and high (right) magnification.

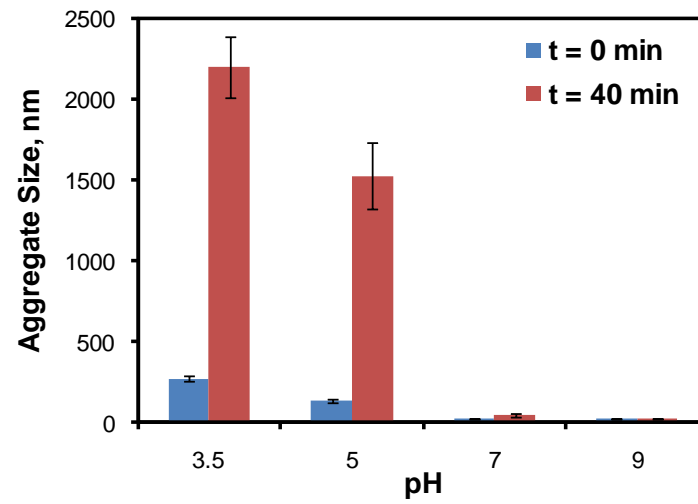


Figure 18: Average aggregate size for a suspension of kaolinite particles as a function of pH.